Journal of Magnetic Resonance **151,** 40–47 (2001)
doi:10.1006/jmre.2001.2338, available online at http://www.idealibrary.com on IDEAL®

Spectral Editing in Solid-State NMR Using Scalar Multiple Quantum Filters

Dimitris Sakellariou,[1] Anne Lesage, and Lyndon Emsley

Laboratoire de Stéréochimie et des Interactions Moléculaires, Ecole Normale Superieure de Lyon, 46 Allée d'Italie, 69364 Lyon, France

E-mail: Lyndon.Emsley@ens-lyon.fr

Received October 3, 2000; revised March 30, 2001

In this paper we describe the use of heteronuclear scalar couplings in solid-state NMR in order to generate multiple-quantum filtering (MQF) pulse sequences. These sequences can be used to edit CP/MAS spectra according to carbon multiplicity. Analytic expressions for the intensity of the MQF signals are obtained using the standard product operator formalism. Experiments that demonstrate the technique are shown in powder samples of camphor and a tripeptide. © 2001 Academic Press

Key Words: **solid-state NMR; spectral editing; *J* couplings; multiple-quantum filters; assignment.**

1. INTRODUCTION

In powder samples, cross polarization (CP), magic angle spinning (MAS), and proton decoupling can yield high-resolution high-sensitivity NMR spectra of dilute spins such as carbon-13 (*1–3*). However, in order for such spectra to be useful in the characterization of molecules in the solid-state, they must be assigned. Complete assignment of natural abundance spectra still presents a considerable challenge. Two-dimensional proton–carbon and proton–nitrogen correlation experiments have been recently shown to be a powerfull approach for the characterization of unlabeled materials (*4*). Alternatively, one-dimensional spectral editing techniques, which identify carbon-13 resonances according to their multiplicity, i.e., the number of directly attached protons, remain a useful tool for the characterization of MAS spectra (*5*). Indeed, in many cases spectral editing when combined with chemical shift analysis is often sufficient to provide an unambiguous characterization in medium-size molecular systems.

Many high-performance techniques are available in liquid-state NMR to perform unambiguous spectral editing, such as INEPT (*6*), APT (*7–11*), and DEPT (*12*). In the solid state one of the most simple and robust techniques is the delayed-decoupling sequence (*13, 14*), which allows resonances to be categorized as either quarternary carbons or other types of carbons (CH_3, CH_2, and CH). Several other schemes have been proposed (*15–27*) to improve this simple technique. Most of them rely on differences between polarization dynamics (and thermodynamics) to differentiate the different multiplicities, and some very subtle techniques have been put forward.

While some of these techniques do perform well, spin diffusion and polarization transfer dynamics can be very complicated and *depend crucially on the mobility and the geometry of the spin system.* Most of the sequences do not work well at moderate to high MAS spinning rates, where spin thermodynamics can be substantially modified, and they are naturally very sensitive to molecular motion, which affects the effective dipolar couplings. This can potentially lead to ambiguities in the assignment of the spectrum using dipolar couplings as a basis for spectral editing (*28*).

An interesting alternative to using the above methods is to use methods analogous to those used in liquids based on scalar couplings. The use of *J* couplings in solids has traditionally been limited to plastic crystals or highly mobile materials (*29, 30*). Recent developments, in particular progress in homonuclear proton–proton dipolar decoupling methods (*31, 32*), have allowed the resolution of heteronuclear *J* couplings in ordinary organic solids (*30, 33*) and consequently their use, as in the liquid state. Notably, the attached proton test (APT) sequence, including appropriate changes for the solid state, has been implemented and been shown to be a reliable technique to perform editing in rigid solids (*33*). The APT sequence leads to the identification of signals based on odd or even multiplicities, and its primary weakness is that it is not entirely straightforward to distinguish CH and CH_3 groups, for example.

In this article we develop a new approach to spectral editing in powdered solids under MAS using heteronuclear scalar couplings to create multiple-quantum (MQ) coherences. Filtering these MQ coherences leads to unambiguous spectral edition. We demonstrate the technique both on a model sample (camphor) and on an ordinary organic compound: a protected synthetic tripeptide.

[1] Present address: Material Sciences Division, Lawrence Berkeley Laboratory, and Department of Chemistry, University of California, Berkeley, California 94720.

1090-7807/01 $35.00

2. THEORY

In a recent publication (*34*) we have shown that heteronuclear double-quantum coherences can be created between a carbon–proton pair and that these are very useful to provide proton–carbon and/or proton–nitrogen (*4*) chemical shift correlation spectra. Here we show that we can extend this approach to higher-order multiple-quantum coherences and use this to filter the carbon spectrum according to the number of attached protons.

In order to evolve under a liquid-state type Hamiltonian, MAS is combined with homonuclear proton decoupling (*35, 36*). Under these conditions the only remaining interactions are the scaled proton chemical shift, the scaled heteronuclear J couplings, and the isotropic carbon chemical shifts. We *assume* that proton–proton J couplings can be neglected, and we *assume* that the homonuclear decoupling sequence is perfect, i.e., it averages out completely the dipolar ^{1}H–^{1}H Hamiltonian. We also *assume* that MAS removes all the anisotropy in the interactions. We are thus left with the liquid type Hamiltonian of the form

$$\mathcal{H} = \delta_S S_z + \lambda \sum_n^N \delta_n^I I_{nz} + \lambda\pi J_{IS} \sum_n^N 2I_{nz}S_z \qquad [1]$$

containing the isotropic chemical shifts δ and the scalar J_{IS} couplings, where the z axis in Eq. [1] of the spin I is the proton dipolar decoupling effective field axis and λ is a scaling factor which depends on the decoupling sequence. In what follows we shall use the scaled coupling $J' \equiv \lambda J$.

This description is of course a simplification. *In practice neither MAS nor the homonuclear decoupling is perfect.* In the limit of "slow" MAS rotation with respect to the cycle time of the multiple-pulse sequence, the time scale of the two averaging effects is well separated. Under these "quasistatic" conditions (*37, 38*), Eq. [1] is valid within the *first*-order approximation in average Hamiltonian theory (*39*) for the radiofrequency averaging. Thus, it should perform reasonably well, even if minor effects arrising from interference with the rotation (*37, 38, 40*) and/or other experimental imperfections are underestimated. To calculate the effects of such nonaveraged higher orders is not trivial. Notably, higher-order terms can yield complex spin diffusion mechanisms (*41*). Here we assume that such effects can be included phenomenologically as a homogeneous T_2 type damping of the coherences. This time constant is taken to be common to all the transitions, although the experimental lineshapes suggest that the outer transitions are in fact broader than the inner ones (*42*). This phenomenological description is a good approximation as long as the real line broadening function has no fine structure (i.e., if it is roughly Gaussian or Lorentzian). If nonzero higher orders give rise to some fine structure in the broadening (i.e., a shift), this will be a complicated function of all parameters (proton and carbon chemical shift anisotropies, dipolar couplings, radiofrequency fields strengths, MAS rates, etc.). In such a case it is reasonable to consider that the effective scaling factor contains some contributions from "unaveraged" dipolar couplings. Because of the r^{-3} dependence of the dipolar couplings, most higher-order effects will be due to nearest neighbors (directly bonded protons), and thus the information about connectivities is not altered. Furthermore, even if higher-order terms are nonzero, the dynamics are governed mostly by scalar J couplings. Finally, the experimentally observed scalar couplings are in good agreement with the expected ones from the liquid state, supporting the argument that any dipolar contribution to the splitting is relatively small.

In summary, in the following we assume liquid-state-like behavior according to Eq. [1] with a damping according to a phenomenological single exponential T_2 dephasing time, where the actual value of the T_2 will depend on experimental features such as ω_r and the performance of the dipolar decoupling sequence. As we shall see, the experimental results are in good agreement with this model, but we do observe effects (notably on the efficiency of the experiments) which probably require a more accurate model to explain.

Special care must be taken in designing the sequence to respect some solid-state features such as the short apparent T_2 dephasing time (even under dipolar decoupling) in the solid state. Thus, for example, we must spend any extended evolution periods with carbon coherence, because the proton coherences dephase too rapidly (a few hundred microseconds). We thus propose the sequence shown in Fig. 1. Note that this experiment is applicable even when a carbon chemical shift distribution leads to an inhomogeneous line broadening, since the π pulse on the carbon channel refocuses this effect. Thus, this technique should be applicable in amorphous solids.

After a first step of magnetization enhancement by cross-polarization for the rare spin S we can generate multiple-spin antiphase coherences with respect to the abundant spin I. Since all terms in the Hamiltonian commute with each other, we can use standard product operator algebra (*43*) and propagate the initial state of the density operator $\sigma_0 = S_x$, at arbitrary time τ:[2]

$$\sigma_0 \xrightarrow{\mathcal{H}\tau} \sigma(\tau). \qquad [2]$$

For the three common organic spin systems, IS, I_2S, and I_3S, after the first τ period and just before the MQ-filter block, (instant τ^- in Fig. 1), we have

$$\sigma_{IS}(\tau^-) = \cos(\pi J'\tau)S_x + \sin(\pi J'\tau)2I_zS_y \qquad [3]$$

$$\sigma_{I_2S}(\tau^-) = \cos^2(\pi J'\tau)S_x + \cos(\pi J'\tau)\sin(\pi J'\tau) \times 2(I_{1z}+I_{2z})S_y - \sin^2(\pi J'\tau)4I_{1z}I_{2z}S_x \qquad [4]$$

$$\sigma_{I_3S}(\tau^-) = \cos^3(\pi J'\tau)S_x + \cos^2(\pi J'\tau)\sin(\pi J'\tau) 2(I_{1z}+I_{2z}+I_{3z})S_y - \cos(\pi J'\tau)\sin^2(\pi J'\tau) \times 4(I_{1z}I_{2z}+I_{1z}I_{3z}+I_{2z}I_{3z})S_x - \sin^3(\pi J'\tau)8I_{1z}I_{2z}I_{3z}S_y. \qquad [5]$$

[2] It is useful to note that the spin S chemical shift is refocused by the π pulse in the middle of the sequence and does not have to be taken into account in the calculations.

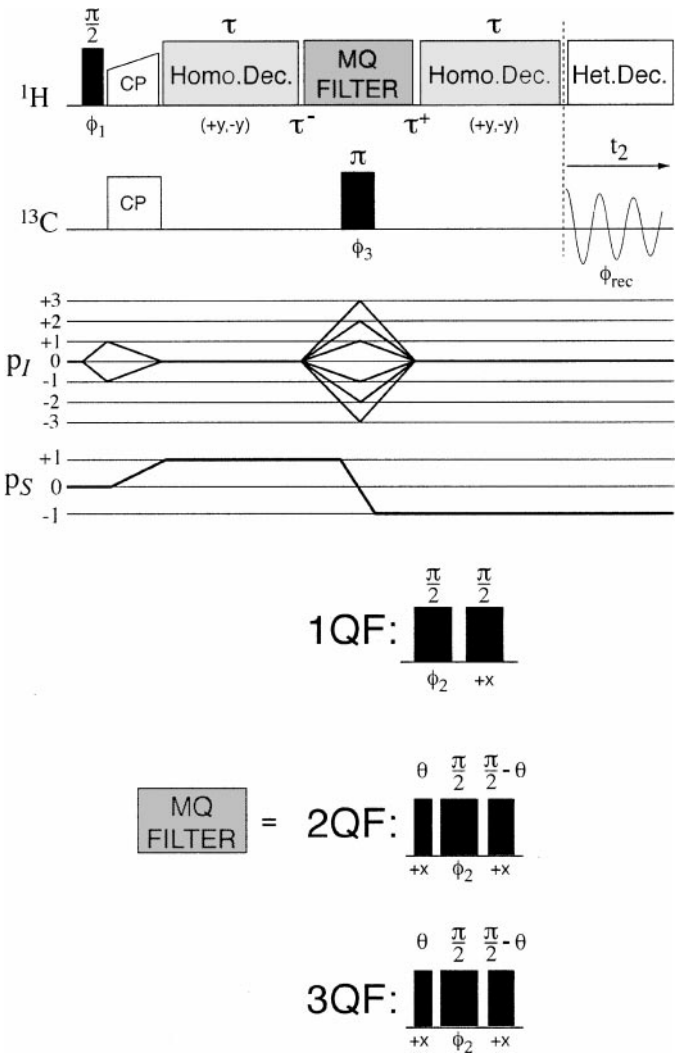

FIG. 1. Pulse sequence and coherence transfer pathways for the *J*-MQ-filter experiment. In our experiments we used the frequency switched Lee-Goldburg (FSLG) (*31*) sequence as the homonuclear proton decoupling scheme, thus θ is a 54.7° pulse. Other homonuclear decoupling sequences can also be used instead of FSLG, by fixing appropriately θ. The phase ϕ_1 was cycled together with the receiver $(+x, -x)$ in order to select carbon magnetization arising only from polarization transfer from protons (spin temperature inversion). The phase ϕ_2 was cycled to select changes of Δ_{PI} according to Table 1. Additional phase cycling on the carbon π pulse is added to suppress artifacts. The MQ-filter block is given at the bottom. For a 1Q-filter only two $\pi/2$ pulses are enough. In fact the first pulse has to be cycled while the phase of the second is constant. We can consider this as a selection of $\Delta_{PI} = \pm 1$ in the frame defined by the effective field of the homonuclear decoupling scheme. The second pulse returns the magnetization parallel to the effective field, ready for the second spin-lock decoupling period. For the 2Q- and 3Q-filters phase cycling in the effective field frame is not obvious. We thus bring the proton magnetization back to the laboratory z axis and then we perform the appropriate phase cycle to select $\Delta_{PI} = \pm 2, \pm 3$, respectively. Finally, as before, the third phase places the magnetization in the plane defined by the effective field. The carbon signal is detected under heteronuclear proton decoupling. In our experiments the two pulse phase modulation (TPPM) (*44*) heteronuclear decoupling scheme was used.

If we chose $\tau = 1/2J'$, we obtain the pure antiphase terms

$$\sigma_{IS}(1/2J') = 2I_zS_y \quad [6]$$

$$\sigma_{I_2S}(1/2J') = -4I_{1z}I_{2z}S_x \quad [7]$$

$$\sigma_{I_3S}(1/2J') = -8I_{1z}I_{2z}I_{3z}S_x \quad [8]$$

Inside the MQ-filter block, multiple-quantum coherences are created by the $\pi/2$ pulse on the I spin, whereas the π pulse on the S spin is used to refocus the S chemical shift after the second τ period. Doing the propagation step by step we have

$$\sigma(\tau^-) \xrightarrow{(\pi/2)I_x} \xrightarrow{\pi S_x} \sigma^{\mathrm{MQ}}. \quad [9]$$

For the three spin systems, we get

$$\sigma_{IS}^{\mathrm{MQ}} = \cos(\pi J'\tau)S_x + \sin(\pi J'\tau)2I_yS_y \quad [10]$$

$$\sigma_{I_2S}^{\mathrm{MQ}} = \cos^2(\pi J'\tau)S_x + \cos(\pi J'\tau)\sin(\pi J'\tau) \times 2(I_{1y} + I_{2y})S_y - \sin^2(\pi J'\tau)4I_{1y}I_{2y}S_x \quad [11]$$

$$\sigma_{I_3S}^{\mathrm{MQ}} = \cos^3(\pi J'\tau)S_x + \cos^2(\pi J'\tau)\sin(\pi J'\tau) \times 2(I_{1y} + I_{2y} + I_{3y})S_y - \cos(\pi J'\tau)\sin^2(\pi J'\tau) \times 4(I_{1y}I_{2y} + I_{1y}I_{3y} + I_{2y}I_{3y})S_x - \sin^3(\pi J'\tau)8I_{1y}I_{2y}I_{3y}S_y. \quad [12]$$

The key idea is to filter out only the signal from particular multiple-quantum coherences. This is performed experimentally using the MQ blocks shown in Fig. 1 and the phase cycling given in Table 1. For a 1Q-filter two $\pi/2$ pulses are sufficient. The first pulse must be cycled while the phase of the second is constant. We can consider this a *selection of* $\Delta_{PI} = \pm 1$ *in the frame defined by the effective field of the homonuclear decoupling scheme*. The second pulse returns the magnetization parallel to the effective field, ready for the second spin-lock decoupling period τ. For the 2Q- and 3Q-filters phase cycling in the effective field frame is not obvious, since more than two phases are required. We thus bring the proton magnetization back to the laboratory z axis and then we perform the appropriate phase cycle to select $\Delta_{PI} = \pm 2, \pm 3$, respectively (*selection in the laboratory frame*). Finally, as before, the third pulse places the magnetization in the plane defined by the effective field.

As a semantic point, note that we deal with a heteronuclear spin system so using a $\Delta_{PI} = \pm 1$ phase cycle (*45*) on the proton channel does not guarantee a change in the total coherence order of $\Delta_{P_{\mathrm{tot}}} = \pm 2$, but it does guarantee the selection of a two-spin coherence. In this example, we cannot (nor do we want to) select only all total double quantum coherences without keeping all total zero quantum coherences. Therefore, in the following *we note the MQ coherences with respect to the coherence order of the spin I.*

TABLE 1
Phase Cycling Schemes for the *J*-MQ-Filter Experiments

	ϕ_1	ϕ_2	ϕ_3	ϕ_{rec}
1QF	0°	0°	{0°, 90°, 180°, 270°}	{0°, 180°, 0°, 180°}
	0°	180°	{0°, 90°, 180°, 270°}	{180°, 0°, 180°, 0°}
	180°	0°	{0°, 90°, 180°, 270°}	{180°, 0°, 180°, 0°}
	180°	180°	{0°, 90°, 180°, 270°}	{0°, 180°, 0°, 180°}
2QF	0°	0°	{0°, 90°, 180°, 270°}	{0°, 180°, 0°, 180°}
	0°	90°	{0°, 90°, 180°, 270°}	{180°, 0°, 180°, 0°}
	0°	180°	{0°, 90°, 180°, 270°}	{0°, 180°, 0°, 180°}
	0°	270°	{0°, 90°, 180°, 270°}	{180°, 0°, 180°, 0°}
	180°	0°	{0°, 90°, 180°, 270°}	{180°, 0°, 180°, 0°}
	180°	90°	{0°, 90°, 180°, 270°}	{0°, 180°, 0°, 180°}
	180°	180°	{0°, 90°, 180°, 270°}	{180°, 0°, 180°, 0°}
	180°	270°	{0°, 90°, 180°, 270°}	{0°, 180°, 0°, 180°}
3QF	0°	0°	{0°, 90°, 180°, 270°}	{0°, 180°, 0°, 180°}
	0°	60°	{0°, 90°, 180°, 270°}	{180°, 0°, 180°, 0°}
	0°	120°	{0°, 90°, 180°, 270°}	{0°, 180°, 0°, 180°}
	0°	180°	{0°, 90°, 180°, 270°}	{180°, 0°, 180°, 0°}
	0°	240°	{0°, 90°, 180°, 270°}	{0°, 180°, 0°, 180°}
	0°	300°	{0°, 90°, 180°, 270°}	{180°, 0°, 180°, 0°}
	180°	0°	{0°, 90°, 180°, 270°}	{180°, 0°, 180°, 0°}
	180°	60°	{0°, 90°, 180°, 270°}	{0°, 180°, 0°, 180°}
	180°	120°	{0°, 90°, 180°, 270°}	{180°, 0°, 180°, 0°}
	180°	180°	{0°, 90°, 180°, 270°}	{0°, 180°, 0°, 180°}
	180°	240°	{0°, 90°, 180°, 270°}	{180°, 0°, 180°, 0°}
	180°	300°	{0°, 90°, 180°, 270°}	{0°, 180°, 0°, 180°}

Note. ϕ_1 is the phase of the first $\pi/2$ proton pulse before the CP step, ϕ_2 is the phase of the first $\pi/2$ proton pulse in the MQ-filter block, and ϕ_3 is the phase of the π carbon pulse (see Fig. 1). ϕ_{rec} is the phase of the receiver for the appropriate MQ filtering. Complete example pulse sequences are available on our website (*46*).

The MQF components for the three-spin systems are easily extracted. For a I one quantum filter,

$$\sigma_{IS}^{1\text{QF}} = \frac{1}{2}\sin(\pi J'\tau)(I_+ - I_-)(S_- - S_+) \quad [13]$$

$$\sigma_{I_2S}^{1\text{QF}} = \frac{1}{2}\cos(\pi J'\tau)\sin(\pi J'\tau) \times (I_{1+} + I_{2+} - I_{1-} - I_{2-})(S_- - S_+) \quad [14]$$

$$\begin{aligned}\sigma_{I_3S}^{1\text{QF}} = {} & \frac{1}{2}\cos^2(\pi J'\tau)\sin(\pi J'\tau)(I_{1+} + I_{2+} + I_{3+} \\ & - I_{1-} - I_{2-} - I_{3-})(S_- - S_+) + \frac{1}{2}\sin^3(\pi J'\tau) \\ & \times (S_- - S_+)[(I_{1+}I_{2-}I_{3-} + I_{1-}I_{2+}I_{3-} + I_{1-}I_{2-}I_{3+} \\ & - I_{1-}I_{2+}I_{3+} - I_{1+}I_{2-}I_{3+} - I_{1+}I_{2+}I_{3-}) \\ & + (I_{1+}I_{2+}I_{3+} - I_{1-}I_{2-}I_{3-})]. \end{aligned} \quad [15]$$

From Eq. [15] we note that the 1QF signal of a CH_3 group also contains 3Q contributions. This is because the phase cycling is unable to distinguish between the two coherence pathways in this case. This does not have significant effects in the editing procedure. For a I two quantum filter we obtain

$$\sigma_{IS}^{2\text{QF}} = 0 \quad [16]$$

$$\sigma_{I_2S}^{2\text{QF}} = \frac{1}{2}\sin^2(\pi J'\tau)(I_{1-}I_{2-} + I_{1+}I_{2+})(S_+ + S_-) \quad [17]$$

$$\begin{aligned}\sigma_{I_3S}^{2\text{QF}} = {} & \frac{1}{2}\cos(\pi J'\tau)\sin^2(\pi J'\tau)(S_+ + S_-)(I_{1-}I_{2-} + I_{1+}I_{2+} \\ & + I_{2-}I_{3-} + I_{2+}I_{3+} + I_{1-}I_{3-} + I_{1+}I_{3+}), \end{aligned} \quad [18]$$

thus, we filter out any CH groups. For a I three quantum filter we have

$$\sigma_{IS}^{3\text{QF}} = 0 \quad [19]$$

$$\sigma_{I_2S}^{3\text{QF}} = 0 \quad [20]$$

$$\sigma_{I_3S}^{3\text{QF}} = \frac{1}{2}\sin^3(\pi J'\tau)(I_{1+}I_{2+}I_{3+} - I_{1-}I_{2-}I_{3-})(S_- - S_+), \quad [21]$$

filtering out all CH and CH_2 groups. The second $\pi/2$ pulse on the I spin converts the multiple quantum coherences into I spin antiphase and the last τ period refocuses the S spin chemical shift and converts the I spin antiphases into S_x observable magnetization detected under heteronuclear decoupling in t_2,

$$\sigma^{\text{MQF}} \xrightarrow{(\pi/2)I_x} \sigma^{\text{MQF}}(\tau^+) \xrightarrow{\mathcal{H}\tau} \sigma^{\text{MQF}}(2\tau), \quad [22]$$

with

$$\sigma_{IS}^{1\text{QF}}(2\tau) = \sin^2(\pi J'\tau)S_x + \cdots \quad [23]$$

$$\sigma_{I_2S}^{1\text{QF}}(2\tau) = \frac{1}{2}\sin^2(2\pi J'\tau)S_x + \cdots \quad [24]$$

$$\sigma_{I_2S}^{2\text{QF}}(2\tau) = \frac{1}{4}\sin^4(\pi J'\tau)S_x + \cdots \quad [25]$$

$$\sigma_{I_3S}^{1\text{QF}}(2\tau) = \frac{1}{2}[3 + 2\cos(2\pi J'\tau) + \cos(4\pi J'\tau)]\sin^2(\pi J'\tau)S_x + \cdots \quad [26]$$

$$\sigma_{I_3S}^{2\text{QF}}(2\tau) = \frac{3}{4}\sin^4(\pi J'\tau)\cos^2(\pi J'\tau)S_x + \cdots \quad [27]$$

$$\sigma_{I_3S}^{3\text{QF}}(2\tau) = \frac{1}{4}\sin^6(\pi J'\tau)S_x + \cdots, \quad [28]$$

where the ellipses account for terms which are not observable. We can include the effect of transverse relaxation phenomenologically during the two τ periods by multiplying the signal by a single exponential. Thus, we obtain the expressions for the observable MQF signals as functions of the initial (after cross-polarization) intensities I^0, relaxation times T_2, and the evolution period τ.

For the single quantum filtered signals,

$$I_{IS}^{1QF}(\tau) = \sin^2(\pi J'\tau)\exp\left(-2\tau/T_2^{IS}\right)I_{IS}^0 \quad [29]$$

$$I_{I_2S}^{1QF}(\tau) = \frac{1}{2}\sin^2(2\pi J'\tau)\exp\left(-2\tau/T_2^{I_2S}\right)I_{I_2S}^0 \quad [30]$$

$$I_{I_3S}^{1QF}(\tau) = \frac{1}{2}[3 + 2\cos(2\pi J'\tau) + \cos(4\pi J'\tau)]\sin^2(\pi J'\tau)] \times \exp\left(-2\tau/T_2^{I_3S}\right)I_{I_3S}^0. \quad [31]$$

For the double quantum filter

$$I_{I_2S}^{2QF}(\tau) = \frac{1}{4}\sin^4(\pi J'\tau)\exp\left(-2\tau/T_2^{I_2S}\right)I_{I_2S}^0 \quad [32]$$

$$I_{I_3S}^{2QF}(\tau) = \frac{3}{4}\sin^4(\pi J'\tau)\cos^2(\pi J'\tau)\exp\left(-2\tau/T_2^{I_3S}\right)I_{I_3S}^0, \quad [33]$$

and for the triple quantum filter

$$I_{I_3S}^{3QF}(2\tau) = \frac{1}{4}\sin^6(\pi J'\tau)\exp\left(-2\tau/T_2^{I_3S}\right)I_{I_3S}^0. \quad [34]$$

In Fig. 2 the dependence of these signals as functions of τ is presented. The curves were calculated for all types of carbon multiplicity and all orders of MQ filtering in the "solid-state" case (Figs. 2d–2f) and compared for reference to the "ideal liquid-state" case (Figs. 2a–2c). In solid samples, the effective scalar coupling is reduced by the scaling factor of the homonuclear decoupling sequence (for FSLG $\lambda = 1/\sqrt{3}$ and a coupling of 130 Hz, which is a typical value for a sp^3 carbon in hydrocarbons (*47*), will give an effective scaled coupling of 75 Hz) and a line broadening of several tens of hertz must be considered, which strongly attenuates the signal intensity by transverse T_2 relaxation. Note that this T_2 is related to the homogenous (not refocusable) linewidth of the carbon resonances. However, if the homonuclear decoupling sequence applied during the 2τ period is efficient enough to yield linewidths comparable to the size of the scaled heteronuclear scalar coupling, then a significant signal should be observed, rendering the experiment practicable. The optimal delay to excite single quantum proton coherences, independent of the number of attached protons, is about 2 ms (Fig. 2d). From the relative intensities of the signals we can see that the 1Q-filter is intrinsically more sensitive than the 2Q- and 3Q-filters. Finite linewidth due to the imperfect decoupling diminishes further the MQ filtered signals, so the efficiency of this technique depends crucially on the efficiency of the homonuclear proton decoupling.

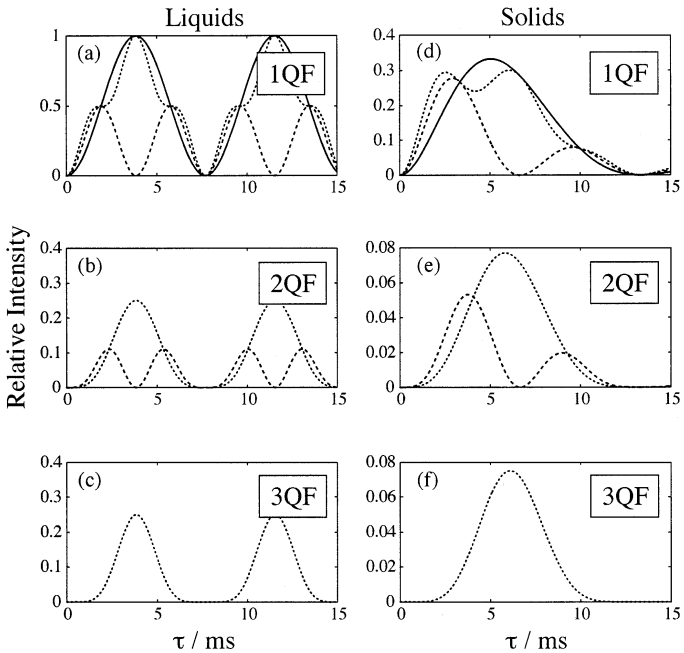

FIG. 2. Functional dependences for MQF signals for the CH (solid line), CH_2 (dashed line), and CH_3 (dotted line) groups. Plots (a, b, c) correspond to the ideal liquid-state evolution where no linewidth is present and the scalar coupling is set to 130 Hz, i.e., a typical value for a one-bond coupling for an aliphatic carbon. Plots (d, e, f) correspond to the solid-state case, where the scalar couplings are scaled by the factor $\lambda = 1/\sqrt{3}$ due to the FSLG decoupling and a finite linewidth exists. In this latter case the linewidth was phenomenologically introduced (see Eqs. [29–34]). T_2 is the transverse relaxation (dephasing) time during the 2τ period ($T_2 = 1/\pi\Delta$) where Δ is the full linewidth at half height of one component in a *J*-coupled multiplet. In this example Δ was set to 30 Hz. Note the differences between liquids and solids with respect to the relative intensities of the signals. The efficiency of the MQ-filters in solids is low because of the fast T_2 damping of the signal.

3. EXPERIMENTAL

In this section we present experimental results using the multiple quantum filters. Powder samples of camphor and the protected tripeptide Boc-Ala-Ala-Pro-O-Bzl were used, in a volume-restricted 4-mm-diameter rotor in a triple resonance CP/MAS probe. The spectra were acquired at a carbon-13 resonance frequency of 125 MHz on a Bruker DSX Avance spectrometer. The sample of camphor was purchased from Sigma and used without further recrystallization. The tripeptide Boc-Ala-Ala-Pro-O-Bzl (where Boc stands for tertbutoxycarbonyl and Bzl for Benzyl) was synthesized in our laboratory and crystallized from diisopropyloxide (*48*).

All pulse programs used are available on our website (*46*). Results for a powder sample of camphor are shown in Fig. 3 and confirm the theoretical predictions. Note that camphor is a plastic crystal, so all intramolecular dipolar couplings are averaged to zero on the NMR time scale (i.e., it would be impossible to perform unambiguous spectral editing using dipolar methods). Clear distinction with respect to the multiplicities of the carbon resonances can be made, especially between the CH and CH_2 carbon resonances. The experimental details are given in the legend to Fig. 3 whereas it is important to note that all four spectra were acquired in less than 60 min.

Clear distinctions for the carbon multiplicities can be made even in rigid organic solids. Figure 4 shows the spectra obtained for the protected tripetide Boc-Ala-Ala-Pro-O-Bzl, together with the experimental details. The complete assignment of the carbon resonances has been given in the literature (*4*). Again, unambiguous assignments for the carbon multiplicities were obtained for this medium-size, natural abundance, organic system (MW 450 g/mol). Using roughly 20 mg of sample, the spectra were obtained in 6, 120, and 240 min, respectively, for the one, two, and three quantum filters, experimental times which are perfectly reasonable for this type of analysis. Although the signal-to-noise ratio is not spectacular, due to the relatively low sensitivity of the technique, its efficiency is in good qualitative agreement with the theoretical predictions discussed above involving a single phenomenological T_2. We do notice some quantitative disparity between relative intensities within a spectrum, but this is not surprising since the phenomenological T_2 is expected to be different for any different multiple quantum coherence order and even for any particular nucleus.

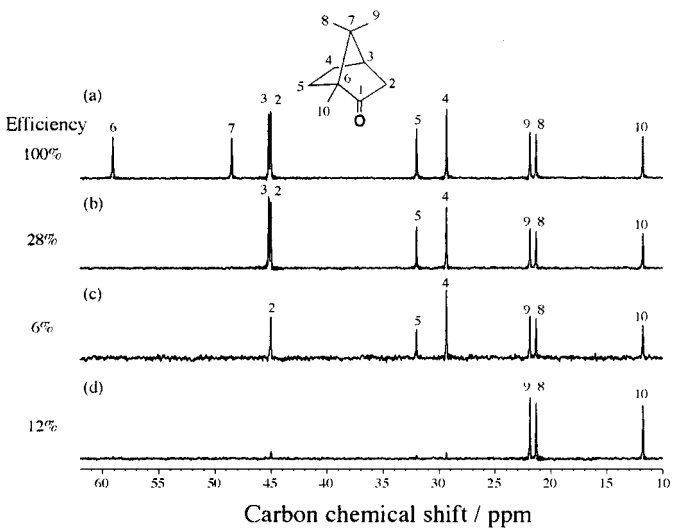

FIG. 3. J-MQ-filtered solid-state NMR spectra for powdered camphor. (a) Standard CP/MAS spectrum of the powder sample of camphor. The spinning frequency was set to 6 kHz and a 5-ms cross-polarization contact time was used. Using TPPM (*44*) heteronuclear decoupling very narrow resonances can be obtained (linewidths less than 2 Hz), so to avoid wiggles due to the truncation of the FID an exponential apodization of 3 Hz was applied. 8 scans were recorded. (b) 1QF spectrum. 64 scans were recorded. As predicted, signals from the CH, CH_2, and CH_3 groups are present. (c) 2QF spectrum. Only signals from the CH_2 and CH_3 groups are present. 128 scans were recorded. The evolution time was set to $\tau = 3.2$ ms for (b) and (c). (d) 3QF spectrum. Only signals from the CH_3 groups are present. The evolution time was set to $\tau = 7.0$ ms in order to enhance the 3Q proton coherences, according to the prediction of Fig. 2f. 480 scans were recorded. The amplitude for the homonuclear and the heteronuclear decoupling RF fields was set to $\omega_1/2\pi = 100$ kHz. In order to quantify the loss of intensity due to the *J*-MQ–filters, the signal-to-noise ratio for the C10 methyl group resonance relative to the CPMAS experiment, corrected for the number of scans, is given next to the spectrum for each experiment. The agreement of the relative intensities with the theoretical predictors of Fig. 2 is excellent.

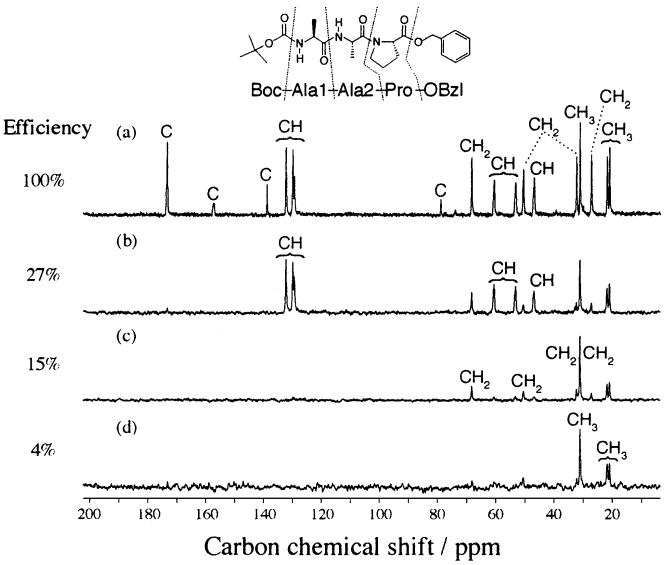

FIG. 4. *J*-MQ-Filtered solid-state NMR spectra of the tripeptide Boc-Ala-Ala-Pro-O-Bzl. (a) Standard CP/MAS spectrum of 20 mg of a powder sample of the tripeptide. The spinning frequency was set to 12.5 kHz and a 1-ms cross-polarization contact time was used. TPPM heteronuclear decoupling ($\omega_1/2\pi = 100$ kHz) was applied during acquisition. 64 scans were recorded. (b) 1Q-Filtered spectrum. As predicted, signals from the CH, CH_2, and CH_3 groups are present. 128 scans were recorded. (c) 2Q-Filtered spectrum. Only signals from the CH_2 and CH_3 groups are present. 2560 scans were recorded. (d) 3Q-Filtered spectrum. Only signals from the CH_3 groups are present. 4800 scans were recorded. The evolution time τ was set to 3.2 ms (synchronized with the MAS) for (b) and (c) and to 7.0 ms for (d) in order to enhance 3Q coherence creation. Spectra (c) and (d) were acquired within 2 and 4 h, respectively. The signal-to-noise ratio relative to the CPMAS experiment, corrected for the number of scans, is given next to the spectrum for each experiment. The signal-to-noise ratio was calculated for the methyl carbon at 31 ppm, and the relative intensities show a good qualitative agreement with the theoretical predictions of Fig. 2.

4. CONCLUSIONS

The *J*-MQ-filtering method for spectral editing appears to be a useful technique to obtain carbon multiplicities in ordinary organic solids. Clear distinction between all carbon multiplicities, and notably between CH and CH_2 groups, are obtained using *J*-MQ-filters. Because the polarization transfer is achieved using scalar coupling, the method is insensitive to molecular mobility and to MAS (as long as the homonuclear decoupling scheme is effective). Note that the relatively low sensitivity of these experiments will increase automatically with the introduction of more efficient decoupling techniques working under faster MAS. Strong radiofrequency fields lead to shorter multipulse cycles and the interference with MAS becomes a less important issue, especially under rotation frequencies close to 20–30 kHz. On the other hand, new rotor-synchronized homonuclear decoupling schemes performing at high MAS frequencies would be a useful building block that can be immediately incorporated in such liquid-like techniques to increase their potential application for spectral characterization in solids.

ACKNOWLEDGMENTS

We are grateful to Dr. Stefan Steuernagel (Bruker) for his technical support during the initial phase of this work and to Prof. J. Vidal (Rennes) for the tripeptide sample. We thank the referees for useful and constructive comments.

REFERENCES

1. A. Pines, M. G. Gibby, and J. S. Waugh, Proton-enhanced nuclear induction spectroscopy. A method for high resolution NMR of dilute spins in solids, *J. Chem. Phys.* **56,** 1776–1777 (1972).
2. A. Pines, M. G. Gibby, and J. S. Waugh, Proton-enhanced NMR of dilute spins in solids, *J. Chem. Phys.* **59,** 569–590 (1973).
3. E. O. Stejskal, J. Schaefer, and J. S. Waugh, Magic-angle spinning and polarization transfer in proton-enhanced NMR, *J. Magn. Reson.* **28,** 105–112 (1977).
4. A. Lesage, P. Charmont, S. Steuernagel, and L. Emsley, Complete resonance assignment of a natural abundance solid peptide by through-bond heteronuclear correlation solid state NMR, *J. Am. Chem. Soc.* **122,** 9739–9744 (2000).
5. K. W. Zilm, "The Encyclopedia of NMR," Wiley, London, 1997.
6. G. A. Morris and R. Freeman, Enhancement of nuclear magnetic resonance signals by polarization transfer, *J. Am. Chem. Soc.* **101,** 760–762 (1979).
7. M. H. Levitt and R. Freeman, Simplification of NMR spectra by masking in a second frequency dimension, *J. Magn. Reson.* **39,** 533–538 (1980).
8. C. LeCocq and J.-Y. Lallemand, Precise carbon-13 NMR multiplicity determination, *J. Chem. Soc. Chem. Commun.* **119,** 150–152 (1981).
9. S. L. Patt and J. N. Shoolery, Attached proton test for carbon-13 NMR, *J. Magn. Reson.* **46,** 535–539 (1982).
10. F.-K. Pei and R. Freeman, A simple scheme for determining multiplicities in carbon-13 NMR spectra, *J. Magn. Reson.* **48,** 318–322 (1982).
11. H. J. Jakobsen, O. W. Sørensen, W. S. Brey, and P. Kanya, The magic angle for the differentiation between CH_3 and CH multiplicities in ^{13}C spin-echo *J*-modulation experiments, *J. Magn. Reson.* **48,** 328–335 (1982).
12. D. T. Pegg, D. M. Doddrell, and M. R. Bendall, Proton-polarization transfer enhancement of a heteronuclear spin multiplet with preservation of phase coherency and relative component intensities, *J. Chem. Phys.* **77,** 2745–2752 (1982).
13. M. Alla and E. Lippmaa, High resolution broad line ^{13}C NMR and relaxation in solid norbornadiene, *Chem. Phys. Lett.* **37,** 260–264 (1976).
14. S. J. Opella and M. H. Frey, Selection of nonprotonated carbon resonances in solid-state nuclear magnetic resonance, *J. Am. Chem. Soc.* **101,** 5854–5856 (1979).
15. E. F. Rybaczewski, B. L. Neff, J. S. Waugh, and J. S. Sherfinski, High resolution ^{13}C in solids: ^{13}C local fields of CH, CH_2 and CH_3, *J. Chem. Phys.* **67,** 1231–1236 (1977).
16. N. C. Nielsen, H. Bildsøe, H. J. Jakobsen, and O. W. Sørensen, SEMUT spectral editing and determination of radiofrequency field strengths for ^{13}C CP/MAS NMR of solids, *J. Magn. Reson.* **79,** 554–560 (1988).
17. G. G. Webb and K. W. Zilm, Asynchronous MASSLF spectroscopy: A convenient method for assigning solid-state carbon-13 CPMAS spectra. *J. Am. Chem. Soc.* **111,** 2455–2463 (1989).
18. N. Sethi, Carbon-13 CP/MAS spectral assignment with one-dimensional separated-local-field spectroscopy., *J. Magn. Reson.* **94,** 352–361 (1991).
19. D. P. Burum and A. Bielecki, WIMSE, a new spectral editing technique for CPMAS solid-state NMR., *J. Magn. Reson.* **95,** 184–190 (1991).
20. X. Wu and K. W. Zilm, Complete spectral editing in CPMAS NMR., *J. Magn. Reson. A* **102,** 205–213 (1993).
21. X. Wu and K. W. Zilm, Methylene-only subspectrum in CPMAS NMR, *J. Magn. Reson. A* **104,** 119–122 (1993).
22. X, Wu, S. T. Burns, and K. W. Zilm, Spectral editing in CPMAS NMR. generating subspectra based on proton multiplicities, *J. Magn. Reson. A* **111,** 29–36 (1994).
23. R. Sangill, N. Rastrup-Andersen, H. Bildsøe, H. J. Jakobsen, and N. C. Nielsen, Optimized spectral editing of ^{13}C MAS spectra of rigid solids using cross-polarization methods, *J. Magn. Reson. A* **107,** 67–78 (1994).
24. J. Peng and L. Frydman, Spectral editing in solid-state MAS NMR using chemical-shift-anisotropy-dephasing techniques, *J. Magn. Reson. A* **113,** 247–250 (1995).
25. P. Rossi, R. Subramanian, and G. S. Harbison, Methylene-only subspectra in ^{13}C CPMAS using a new double quantum filtering sequence, *J. Magn. Reson.* **141,** 159–163 (1999).
26. J. Z. Hu, J. Harper, C. Taylor, R. J. Pugmire, and D. M. Grant, Modified spectral editing methods for ^{13}C CP/MAS experiments in solids, *J. Magn. Reson.* **142,** 326–330 (2000).
27. S. T. Burns, X. Wu, and K. W. Zilm, Improvement of spectral editing in solids: A sequence for obtaining $^{13}CH + {}^{13}CH_2$-only ^{13}C spectra, *J. Magn. Reson.* **143,** 352–359 (2000).
28. A. Lesage, M. Bardet, and L. Emsley, Through-bond carbon–carbon connectivities in disordered solids by NMR, *J. Am Chem. Soc.* **121,** 10987–10993 (1999).
29. T. Terao, H. Miura, and A. Saika, High-resolution *J*-resolved NMR spectra of dilute spins in solids, *J. Chem. Phys.* **75,** 1573–1574 (1981).
30. K. W. Zilm and D. M. Grant, High-resolution NMR spectra with *J* couplings in solids, *J. Magn. Reson.* **48,** 524–526 (1982).
31. A. Bielecki, A. C. Kolbert, and M. H. Levitt, Frequency-switched pulse sequences: Homonuclear decoupling and dilute spin NMR in solids, *Chem. Phys. Lett.* **155,** 341–346 (1989).
32. D. Sakellariou, A. Lesage, P. Hodgkinson, and L. Emsley, Homonuclear dipolar decoupling in solid-state NMR using continuous phase modulation, *Chem. Phys. Lett.* **319,** 253–260 (2000).
33. A. Lesage, S. Steuernagel, and L. Emsley, Carbon-13 spectral editing in solid-state NMR using heteronuclear scalar couplings, *J. Am. Chem. Soc.* **120,** 7095–7100 (1998).
34. A. Lesage, D. Sakellariou, S. Steuernagel, and L. Emsley, Carbon–proton chemical shift correlation in solid-state NMR by through-bond multiple-quantum spectroscopy, *J. Am. Chem. Soc.* **120,** 13194–13201 (1998).
35. T. Terao and S. Matshui, Indirectly induced NMR spin echoes in solids, *Phys. Rev. B* **21,** 3781–3784 (1980).
36. H. Miura, T. Terao, and A. Saika, NMR spectra of dilute spins under slow sample-spinning and homonuclear decoupling, *J. Chem. Phys.* **85,** 2458–2462 (1986).
37. D. E. Demco, S. Hafner, and H. W. Spiess, Rotation-synchronized homonuclear dipolar decoupling, *J. Magn. Reson. A* **116,** 36–45 (1995).
38. S. Hafner and H. W. Spiess, Multiple-pulse line narrowing under fast magic-angle spinning, *J. Magn. Reson. A* **121,** 160–166 (1996).
39. U. Haeberlen and J. S. Waugh, Coherent averaging effects in magnetic resonance., *Phys. Rev.* **175,** 453–467 (1968).
40. C. Filip and S. Hafner, Analysis of multiple-pulse techniques under fast MAS conditions, *J. Magn. Reson.* **147,** 250–260 (2000).
41. M. Hohwy, C. P. Jaroniec, B. Reif, C. M. Rienstra, and R. G. Griffin, Local structure and relaxation in solid-state NMR: Accurate measurement of amide N–H bond lengths and H–N–H bond angles. *J. Am. Chem. Soc.* **122,** 3218–3219 (2000).

42. D. Sakellariou, "Development of New Methods for High Resolution in Nuclear Magnetic Resonance of Solids," Ph.D. Thesis, ENS, Lyon, 2000.

43. O. W. Sørensen, G. W. Eich, M. H. Levitt, G. Bodenhausen, and R. R. Ernst, Product operator formalism for the description of NMR pulse experiments, *Progr. NMR Spectrosc.* **16,** 163–192 (1983).

44. A. E. Bennett, C. M. Rienstra, M. Auger, K. V. Lakshmi, and R. G. Griffin, Heteronuclear decoupling in rotating solids, *J. Chem. Phys.* **103,** 6951–6958 (1995).

45. R. R. Ernst, G. Bodenhausen, and A. Wokaun, "Principles of Nuclear Magnetic Resonance in One and Two Dimensions," Clarendon Press, Oxford, 1989.

46. Http://www.ens-lyon.fr/STIM/NMR/.

47. H. O. Kalinowski, S. Berger, and S. Braun, "Carbon-13 NMR Spectroscopy," Wiley, Chichester, 1988.

48. L. Guy, J. Vidal, A. Collet, A. Amour, and M. Reboud-Ravaux, Design and synthesis of hydrazinopeptides and their evaluation as human leucocyte elastase inhibitors, *J. Med. Chem*. **41,** 4833–4843 (1998).